Carpathian Journal of Earth and Environmental Sciences, November 2013, Vol. 8, No. 4, p. 209 - 220

GEOCHEMICAL AND Sr, Nd ISOTOPIC SIGNIFICANCE OF POST-COLLISIONAL KEBAN A-TYPE SYENITES, ELAZIĞ, SOUTHEASTERN TURKEY

Sevcan KÜRÜM

University of Fırat, Engineering Faculty, Department of Geology, Elazığ, Turkey, skurum@firat.edu.tr

Abstract: The Cretaceous age plutons with shoshonite affinity occurring in the Keban region (Northwest Elazığ in Southeast Anatolia) display A-type magma characteristics (e.g., Nb+Ce+Y+Zr > 400 ppm, Na_2O+K_2O > 8 wt.%). The intrusive bodies comprise syenitic, with rare granodioritic, porphyries. They consist of predominantly K-feldspar and plagioclase, with lesser quartz, amphibole, biotite and pyroxene phenocrysts, and of accessory minerals such as apatite, zircon and zeolite. The plutons are highly enriched in LREE and show significant negative Ba, Nb, Sr and Ti anomalies. Changes in separated K-feldspar crystals (Kfm) (87Sr/86Sr 0.70609-0.70610) and whole rock Sr-Nd (87Sr/86Sr 0.70597-0.70628) isotope composition in terms of some elements and major oxides indicate that fractional crystallisation process took place during the crystallisation of these minerals and rocks. The 143Nd/144Nd ratio measured in one single Kfm sample was 0.51243 which was similar to the 143Nd/144Nd values of 0.51238-0.51242 obtained from the whole rocks. Geochemical and isotopic variations of A-type syenites bearing K-feldspar megacrystals (Kfm) are consistent with those of the lithospheric mantle (EMII) and crustal sources that were modified by subduction zone enrichment. Nd/La (0.4 – 0.8) and Nb/Y (0.45-1.1) ratios imply the role of astenospheric fluids in their origin. The within-plate and late orogenic tectonic settings described in the tectonic discrimination diagrams are conformable with those of A-type magmas. The proposed model supports the fact that the partial melting of both crustal and subduction-modified chemically enriched subcontinental lithospheric sources, which was triggered by an upwelling asthenosphere and underplating, played a significant role in the genesis of Keban A-type syenites. Data also suggests that the A-type Keban syenites are likely formed within the Southeast Anatolian extension-related tectonic system that arosed post- collision of the Eurasia and Arabian plates.

Keywords: A-type syenite, Sr-Nd isotope geochemistry, lithospheric mantle, post-collisional, Keban-Elazığ, SE Turkey

1. INTRODUCTION

Understanding of the nature of magmatism within the orogenic belts is important to characterize the geodynamic setting. A-type granitoids have particular importance for the geodynamic interpretations because of their unique mineralogical and geochemical features (Whalen et al. 1987; Martin, 2006; Yang et al. 2006; and Bonin, 2007). A-type granitoids consist of rocks from Q-syenites to peralkaline granites and their volcanic equivalents (Eby, 1990). Eby (1992) has divided them into two groups based on their chemical properties. According to Eby (1992), A_1 granitoids display an element distribution similar to that of island basalts and they may be formed as a result of the differentiation of magma originating from a single source like that of oceanic island basalts but located in the continental rifts. A_2 granitoids are the products of magma formed during continental collision or the collision of continental crust or from magma of underplated crust origin formed as a result of island arc magmatism. Based on his studies in Alaskan Cordillera, The New England and Lachlan Fold Belts of Australia and The Arabian-Nubian Shield, Sylvester (1989) uses A-type or highly fractioned felsic I-type granite terms for the alkaline granites and suggests that these granitoids were formed as a result of post-collisional plate tectonic events.

There are magmatic rocks in the Keban region (NW Elazig, SE Anatolia), which are located in the SE Anatolian orogenic belt. A-type High-K syenitic rocks in the area of Keban are found within the magmatism found in the SE Anatolian orogenic belt.

This magmatism is considered to be a natural result of the closing of the Neothethys Ocean beginning in the Late Cretaceous and the continental collision of the Eurasian and Afro-Arabian plates and post-collision events (Yılmaz, 1993; Kuşçu et al., 2007, 2010). It is also accepted that the magmatism and mineralization events occurred during this period between 82.90+-0.43Ma and 44.43+-0.61 Ma, when the roll-back of subduction and collision, slab rupture and STEP (Subduction-Transfer-Edge-Propagator) mechanisms were predominant (Kuşçu et al., 2007).

In the region, two different magmatisms occurred during the Mesozoic-Cenozoic ages. The first magmatism (calc-alkaline) around the areas of Elazığ, Malatya and further west Kahramanmaraş intruded into the Malatya-Keban metamorphic massives and the Göksun, Berit, İspendere and Kömürhan ophiolites (Parlak, 2006; Rızaoğlu et al., 2008). The second was the calc-alkaline-alkaline magmatism located in the same geological belt as the first one with the age of Late Cretaceous – Middle Eocene (Kuşçu et al., 2007). Kuşçu et al., (2007) claim that these calc alkaline-alkaline magmatites are 69 Ma old in the Keban area and gets younger towards the North.

The objectives of this study are to reinvestigate the geochemical properties of the syenitic intrusive rocks containing abundant K-feldspar megacrytals in order to discuss the origin of Kfms and host rocks and to contribute to the evaluation of the petrogenetic processes caused by the regional extension while taking the previous studies into consideration (Çalık & Öngen, 1998; Parlak, 2006; Rızaoğlu et al., 2008; Kürüm, 2012).

2. GEOLOGY AND STRATIGRAPHY

The studied area is situated in the Eastern Taurid orogenic belt where the basement rocks are the Keban Metaorphic rocks of Paleozoic age. The Keban Metaorphic rocks consist of formations with different lithologies (Kipman, 1983; Çalık & Öngen 1998) (Fig. 1). This metamorphic massif that was subjected to medium- and low-grade metamorphism is widespread in the region. The Keban area is considered to be a place where the syenitic rocks are abundant (Kipman, 1983; Çalık and Öngen, 1998). The Cretaceous age syenitic intrusive rocks are distributed along a nearly north–south line and are found as independent outcrops of various sizes. One of the most prominent properties of these alkaline syenitic rocks, which were intruded in the Keban metamorphic rocks with intrusive contacts and contact relationships with almost all units of the metamorhpites, is their abundant K-feldspar megacrystals. The youngest units found in the studied area are in the Alibonca Formation of the Early Miocene age. The outcrops are limited to the northeast of the studied area (Fig. 1).

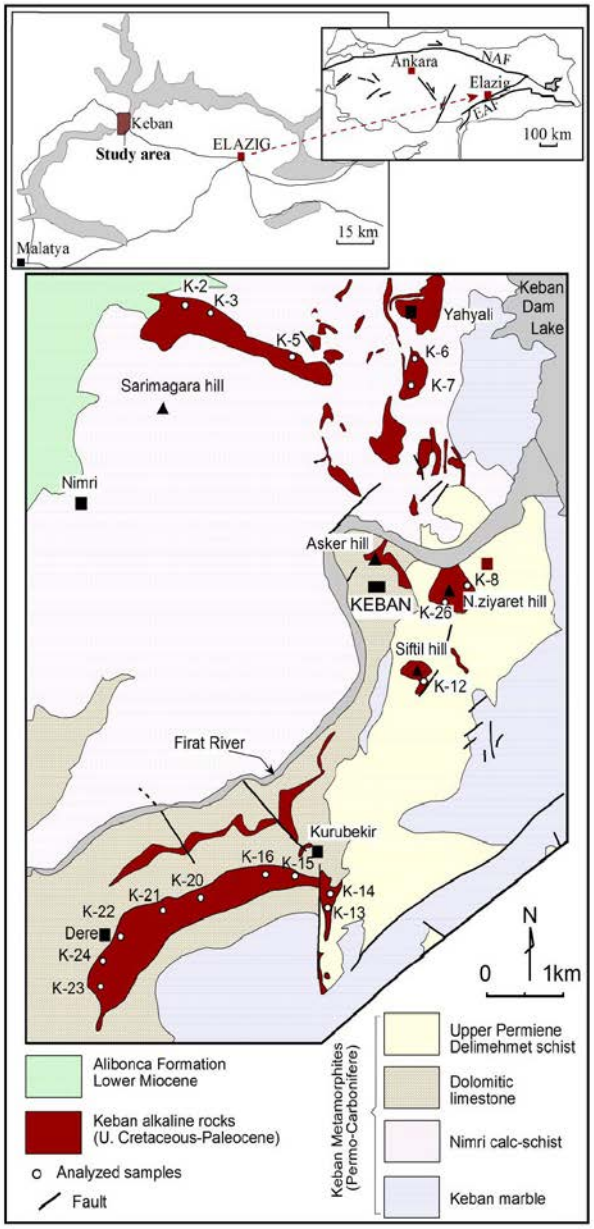

Figure 1. Geological map and location maps of the Keban area and A–type Keban syenitic rocks (Kürüm, 2012). NAF–EAF: North–East Anatolian Fault.

3. ANALYTICAL TECHNIQUES

The whole rock analyses of the 15 rock samples and the mineral chemistry of 5 Kfm used in this study was taken from Kürüm (2012). In addition, major, minor and REE analyses of 3 Kfm samples were made in the scope of this study.

The Kfms major and trace elements were determined by ICP-emission spectrometry and ICP-mass spectrometry using standard techniques at ACME, Analytical Laboratories Ltd., Vancouver,

Canada. 0.2 g of rock and Kfm-powder was fused with 1.5 g $LiBO_2$ and dissolved in 100 ml 5% HNO_3. Loss on ignition (LOI) was determined on dried samples heated to a temperature of 1000°C. REE analyses were performed by ICP-MS at ACME. Detection limits ranged from 0.01 to 0.1 wt % for major oxides, from 0.1 to 10 ppm for trace elements and from 0.01 to 0.5 ppm for REE.

Isotopic analyses were performed at the Radiogenic Isotope Laboratory of METU Central Laboratory in a similar manner to the analytical procedures described by Romer et al. (2001). Isotope ratios were measured using a Triton Multi-Collector Thermal Ionization Mass Spectrometer. Sr was separated in a 2.5 N HCl medium using 12 ml Bio Rad polypropylene columns with 2 ml Bio Rad 100–200 mesh AG50 W-X12 resin. Sr was loaded on single Re-filaments with Ta-activator and 0.005 N H_3PO_4, and its isotopic composition was determined by using static multicollection. Analytical uncertainties were about 2δm level. $^{87}Sr/^{86}Sr$ data were normalized with $^{86}Sr/^{88}Sr= 0.1194$. During the course of the measurement Sr standard NIST SRM 987 was measured as 0.710247 ± 10 (n=3), which is within the accepted range of error for this standard.

A REE fraction was collected from the cation exchange columns with 6 N HCl after Sr was separated. Nd was separated from the REE fraction in a 0.022 N HCl medium using 12 ml Bio Rad poly propylene columns with 2 ml biobeads (Bio Rad) coated with HDEHP (bisethyexyl phosphate). Nd was loaded on double Refilaments with 0.005 N H_3PO_4 and its isotopic composition was determined by using static multicollection. $^{143}Nd/^{144}Nd$ data were normalized to $^{146}Nd/^{144}Nd= 0.7219$. Measurement of the Nd La Jolla standard gave a value of 0.511846 ± 5 (n= 3), which is within the accepted error range for this standard. No corrections were applied to Nd and Sr isotopic compositions for instrumental bias.

4. PETROGRAPHY AND MINERALOGY

Petrographically these intrusive rocks arealkaline syenite porphyry, syenite porphyry and monzonite porphyry in composition (Kürüm, 2012). The main components of these rocks are K-feldspars and plagioclases, and they generally display phaneritic-porphyric and to a lesser trachitoidic texture. The mafic mineral content of these rocks is low. Besides the main components, they contain quartz, amphibole, biotite, pyroxene, sphene, apatite, zircon and zeolite as accessory minerals. K-feldspar, which is the main component of these rocks, is usually found as megacryst, phenocryst and microlite, and locally forms growth structures in plagioclases and K-feldspars. The K-feldspars usually contain orthoclase, plagioclase, rutile, zircon, amphibole, sphene and magnetite inclusions. Many plagioclase inclusions were chemically analysed and the results indicated that they were of oligoclase and andesine in composition (An 16-30%) (Kürüm, 2012). The Carlsbad-simple twinning seen in the Kfms (Kürüm, 2012) indicates that these are shallow intrusive rocks (Vernon, 1986). In all of these samples, the major elements of Kfms display an irregular distribution, indicating an oscillatory zonation. Mineral calculations based on all these element distributions in Kfms indicate that 66-86% of all the Kfms are of orthoclase in composition (when the analysed 27-47 points were taken into consideration (Kürüm, 2012).

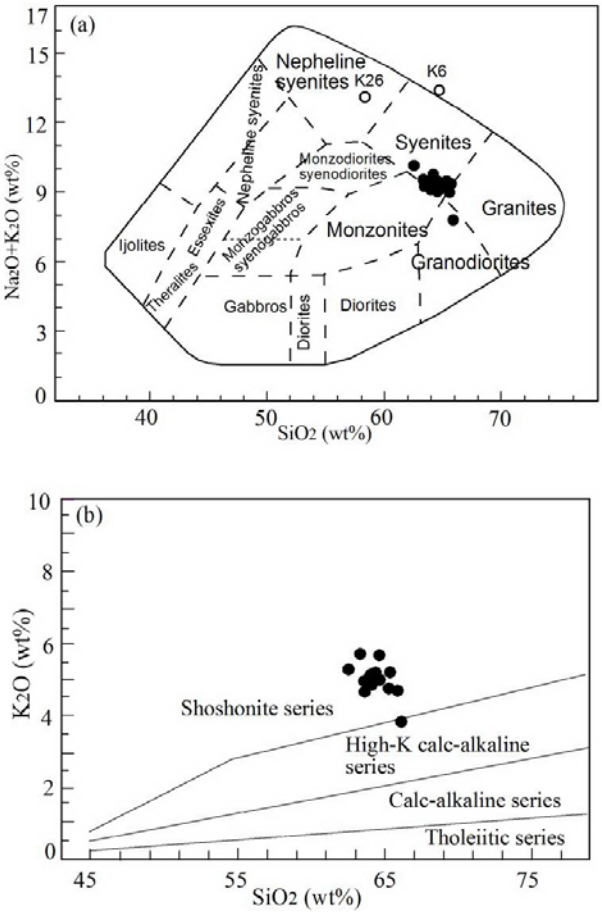

Figure 2. Major element geochemical discrimination diagrams of the Keban alkaline rocks (a) Total alkalis vs silica (after MacKenzie et al., 1982), (b) K2O vs silica (after Pecerillo & Taylor, 1976).

5. WHOLE-ROCK GEOCHEMISTRY

Major, trace and REE analyses from the fifteen whole rocks and three Kfms are given in table 1. Tables 1 and 2 the SiO_2 contents of the analysed samples vary between 62 and 66% and are similar to each other except for sample K26.

Table 1. Whole-rock major element (wt%) and trace element (ppm) chemical analysis results of the Keban syenitic intrusive rocks and Kfms.

	Rock															Mineral		
Sample	K2	K3	K5	K6	K7	K8	K12	K13	K15	K16	K20	K21	K22	K24	K26	K7	K12	K20
SiO_2	64.52	63.47	63.25	64.59	65.94	64.54	63.44	63.91	63.84	65.21	65.77	65.25	64.09	64.16	58.20	62.85	63.01	63.63
Al_2O_3	17.15	16,11	16,07	16,32	16,34	15,58	16,94	15,78	16,02	16,15	15,54	16,45	16,23	16,35	16,62	18.82	19.72	19.48
Fe_2O_3	2,92	3,03	2,94	1,19	2,30	2,05	2,56	2,36	2,91	2,19	2,59	2,92	3,01	2,81	2,00	0.37	0.51	0.47
MgO	0,54	0,21	0,66	0,11	0,26	0,71	0,24	0,55	0,18	0,19	0,54	0,28	0,15	0,17	0,49	0.02	0.05	0.05
CaO	1,79	3,81	2,93	1,68	3,18	3,16	3,78	4,18	3,84	3,47	3,22	2,38	3,68	3,59	3,97	1.37	1.10	0.86
Na_2O	4,39	4,82	3,63	0,81	4,09	3,74	4,96	4,26	4,42	4,53	4,38	4,19	4,51	4,72	0,51	3.19	4.13	3.71
K_2O	4,92	4,62	5,64	12,63	3,78	5,60	5,23	4,91	4,90	4,68	4,62	5,17	4,89	4,96	12,67	10.75	9.21	9.94
TiO_2	0,32	0,32	0,31	0,17	0,23	0,26	0,26	0,31	0,28	0,28	0,32	0,28	0,27	0,28	0,25	0.05	0.04	0.05
P_2O_5	0,11	0,12	0,12	0,05	0,09	0,15	0,09	0,13	0,09	0,10	0,17	0,08	0,09	0,08	0,09	0.01	0.01	0.01
MnO	0,01	0,06	0,05	0,03	0,03	0,06	0,04	0,04	0,05	0,05	0,04	0,03	0,05	0,05	0,06	0.01	0.01	0.01
LOI	2.8	2.9	4.0	1.9	3.4	3.8	2.9	3.1	2.9	2.6	2.4	2.4	2.5	2.3	4.7	1.3	0.8	0.5
Ni	<20	<20	<20	<20	5.9	12.7	<20	<20	<20	<20	<20	<20	<20	<20	10.0	19	18	19
Co	4,6	4,5	2,3	0,8	1,3	2,0	1,4	4,2	1,9	3,0	3,3	5,1	1,8	2,6	1,4	0.3	0.3	0.7
V	52,0	53,0	52,0	24,0	37,0	40,0	49,0	45,0	45,0	47,0	46,0	45,0	45,0	45,0	52,0	17	18	17
Cu	4,2	4,2	4,0	21,1	1,9	7,6	4,5	4,9	3,9	3,6	4,6	2,4	2,8	3,1	103,1	1.3	1.9	1.2
Pb	7,0	4,4	7,3	8,7	1,9	5,1	14,8	5,4	14,7	11,0	5,3	11,9	15,4	37,9	6,2	1.4	6.4	0.9
Zn	30	30	18	12	11	34	13	14	15	12	10	20	23	17	24	6	9	3
Bi	0.2	0.1	0.2	0.1	0.1	0.3	0.4	0.3	0.5	0.2	0.2	0.2	0.3	0.2	0.2	0.1	0.1	0.1
W	3,2	3,6	19,2	48,1	9,6	10,4	4,5	6,0	8,8	6,6	4,9	7,5	6,8	1,9	17,5	1.1	1.1	0.5
Mo	0.9	0.2	2.6	1.1	0.6	0.4	0.5	0.3	0.3	0.5	0.3	0.3	0.3	0.4	0.8	0.3	0.4	0.2
As	2.9	6.6	3.7	3.7	5.0	7.4	2.7	2.1	4.2	2.6	1.5	3.5	4.0	2.9	2.6	0.8	1.1	0.4
Sb	0.2	0.3	0.6	2.0	0.2	0.6	0.3	0.2	0.6	0.2	0.2	0.4	0.5	0.5	0.7	0.1	0.2	0.1
Rb	145	144	212	369	124	213	176	155	189	188	158	194	162	166	332	198	170	184
Cs	6.3	6.2	18.3	4.8	3.9	3.9	3.8	2.6	3.4	2.6	2.3	2.4	3.3	4.7	7.4	1.0	3.4	0.7
Ba	2494	2158	2161	3938	1149	1592	2472	2009	2461	2219	1951	2527	2332	2575	2823	9241	9328	9214
Sr	1383	1537	952	379	1087	746	1485	1298	1615	1603	1318	1605	1642	1638	597	2124	3100	2530
Ga	21.0	20.2	20.3	21.2	20.0	19.3	20.9	19.1	20.5	21.5	19.1	21.0	20.8	20.0	19.9	17.3	17.7	16.9
Ta	2.4	2.4	2.7	1.2	2.1	2.0	2.6	2.1	2.0	2.0	2.2	1.6	2.0	1.9	2.2	0.5	0.4	0.4
Nb	47.3	50.6	47.8	40.2	40.8	41.2	57.3	42.8	39.5	40.6	41.1	38.5	38.3	37.3	48.3	7.3	6.3	6.5
Hf	10.6	11.2	11.0	9.9	9.6	8.4	13.4	9.4	10.4	11.9	9.8	10.6	10.5	10.2	11.8	1.9	1.1	2.0
Zr	345	373	356	335	320	294	443	319	380	412	320	377	380	357	387	64	30	78
Y	20.1	21.3	20.2	8.6	21.4	18.1	21.5	18.6	23.6	27.7	17.8	29.1	24.3	22.9	19.6	2.6	2.0	3.6
Th	81.1	83.4	79.0	90.9	62.9	58.7	88.8	65.6	97.3	102.3	63.8	98.8	99.1	95.9	81.6	6.1	5.0	5.6
U	6.2	8.5	22.6	20.0	16.7	18.6	23.1	22.5	30.2	24.0	19.1	15.5	33.2	33.5	21.2	2.5	1.4	3.6
Ba/Nb	52.73	42.65	45.21	97.96	28.16	38.64	43.14	46.94	62.30	54.66	47.47	65.64	60.89	69.03	58.45	-	-	-
Na_2O+K_2O	9.31	9.44	9.27	13.44	7.87	9.34	10.19	9.17	9.32	9.21	9.00	9.36	9.40	9.68	13.18	13,94	13,34	13,65
Rock samples fron Kürüm, 2012																		

Table 2. RRE (ppm) results of the Keban syenitic intrusive rocks and Kfms.

	Rock														Mineral		
Sample	**K2**	**K3**	**K5**	**K6**	**K7**	**K8**	**K12**	**K13**	**K15**	**K16**	**K20**	**K21**	**K22**	**K24**	**K26**	**K7**	**K12**	**K20**
SiO_2	64.52	63.47	63.25	64.59	65.94	64.54	63.44	63.91	63.84	65.21	65.77	65.25	64.09	64.16	58.20	62.85	63.01	63.63
La	80.60	86.30	81.60	46.60	78.90	67.50	80.60	72.70	96.40	126.5	67.40	122.9	107.7	106.8	28.00	7.90	9.3	8.9
Ce	123.4	150.50	144.4	81.50	117.3	119.8	143.9	131.3	167.3	209.5	122.1	141.8	189.7	186.8	69.40	12.90	16.2	16.7
Pr	15.30	16.30	15.50	8.20	14.40	12.60	15.60	14.00	18.20	22.30	13.20	21.00	20.00	19.40	9.50	1.47	1.71	1.84
Nd	51.70	55.00	53.00	25.70	48.70	42.40	53.20	48.10	61.80	72.30	46.90	71.40	65.80	65.40	38.30	5.50	5.8	7.4
Sm	7.34	7.88	7.72	3.36	7.04	6.11	8.29	6.94	8.71	10.14	6.76	9.81	9.09	9.12	7.01	0.89	0.99	1.21
Eu	1.71	1.74	1.67	0.69	1.60	1.39	1.80	1.50	1.99	2.15	1.48	2.19	1.98	2.02	1.43	1.02	1.08	1.08
Gd	5.13	5.26	5.10	2.25	5.16	4.25	5.70	1.65	5.96	5.68	4.51	7.14	6.06	6.00	5.14	0.67	0.70	0.92
Tb	0.71	0.74	0.72	0.30	0.72	0.59	0.76	0.65	0.80	0.91	0.62	0.93	0.81	0.82	0.71	0.11	0.10	0.13
Dy	3.46	3.72	3.35	1.50	3.51	2.92	3.64	3.12	3.85	4.33	2.90	4.43	3.93	4.00	3.38	0.48	0.45	0.62
Ho	0.64	0.65	0.65	0.29	0.66	0.54	0.66	0.58	0.74	0.80	0.56	0.85	0.74	0.71	0.61	0.09	0.08	0.12
Er	1.74	1.89	1.76	0.80	1.78	1.49	1.80	1.51	2.09	2.25	1.50	2.32	2.05	2.07	1.67	0.26	0.20	0.35
Tm	0.26	0.29	0.27	0.13	0.28	0.24	0.27	0.24	0.33	0.36	0.24	0.36	0.33	0.32	0.25	0.05	0.03	0.06
Yb	1.75	1.90	1.96	0.81	1.73	1.57	1.75	1.61	2.14	2.40	1.52	2.25	2.27	2.08	1.65	0.29	0.19	0.34
Lu	0.26	0.30	0.28	0.13	0.26	0.23	0.26	0.24	0.32	0.37	0.23	0.36	0.34	0.32	0.23	0.04	0.01	0.03
La/Yb_N	31.29	30.86	28.28	39.08	30.98	29.21	31.29	30.68	30.60	35.81	30.12	37.11	32.23	34.88	11.53	18.51	33.25	17.78
Eu/Eu*	0.61	0.60	0.59	0.43	0.57	0.57	0.59	0.57	0.61	0.61	0.57	0.61	0.61	0.62	0.51	1.34	1.38	1.19

Rock samples from Kürüm, 2012

The values of Na_2O and K_2O vary from 3 to 5% and 4 to 6%, respectively, with some deviations contents ignored. The rock samples were concentrated in the syenite area close to the granite, granodiorite and monzonite areas in the total alkali-silica (TAS) diagram (Fig. 2a) (MacKenzie et al., 1982). Syenites (excluding 1 sample) display a High-K, shoshonitic trend in the K_2O-SiO_2 diagram (Fig. 2b) (Pecerillo & Taylor, 1976). The samples K6 (12.63) and K26 (12.67) are not shown in figure 2b because of their higher K2O (%) concentrations. These rocks with a low alumina index show metaluminous affinity. Some of the characteristic chemical properties of the A-type granitoids (Eby, 1990): They have high total alkalies (average Na_2O+K_2O is 9.81), low CaO content (at SiO_2=70%, CaO< 1.8%) (Eby, 1990) and high FeO^t/MgO (average 9.7) and Zr+Nb+Ce+Y (> 400 ppm).

Figure 3. (a) Fe2O3t / MgO vs. Zr+Nb+Ce+Y, and (b) Zr vs. 10.000 Ga/Al discrimination diagrams of Whalen at al. (1987), A-type Keban syenitic rocks.

The variation diagrams of Whalen et al. (1987) (Figs. 3a-b), based on some major oxide and trace elements of the samples, also indicate that these samples are of A-type granitoid property. The chemical properties of these rocks indicate their relative poorness in mafic minerals. These results are in harmony with the petrographic data (Kürüm, 2012).The fact that LREE are enriched compared to

HREE and $La/Yb)_N$ ratios, which are usually high (39.08-29.21) as shown in the chondrite normalized diagram of the rock samples (Fig. 4a) (normalizing values taken from Sun & McDonough, 1989), indicates a fractionation between LREE and HREE. The samples also display a very weak Eu anomaly (Eu/Eu*=0.43-0.62) (Fig. 4a). The sample K-26 shows the different nature in this figure. Thise sample falls into the nepheline syenite area in the nomenclature diagram (Figure 2a). Its LOI value is relatively higher than other samples.

The primitive mantle normalized (Sun & McDonough, 1989) samples display an enrichment in U and Th, depletion in Nb and a negative anomaly for Ti (Fig. 4b). The diagram also shows light to medium HFSE and REE enrichment and HREE depletion.

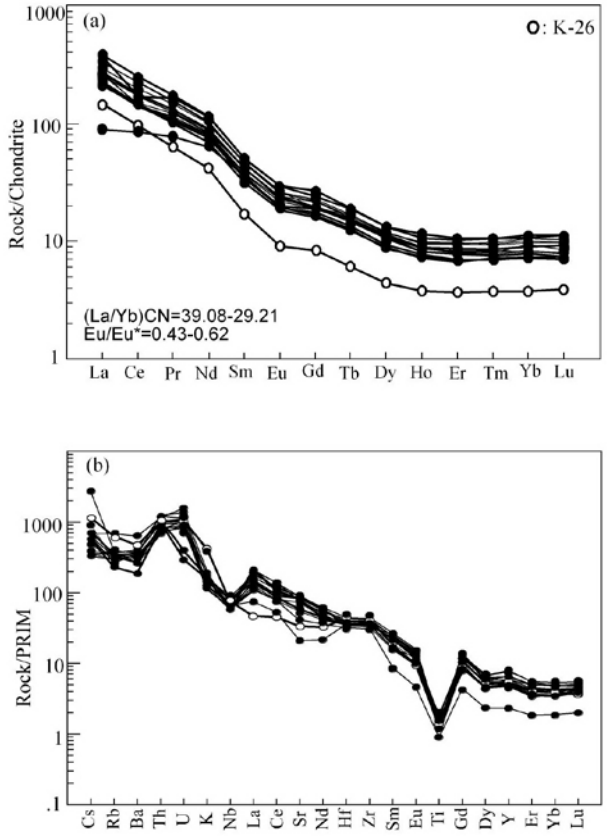

Figure 4. (a) Chondrite-normalized REE and (b) primitive mantle normalized trace element spider diagram of the Keban alkaline rocks. Normalization values after Sun and McDonough (1989).

6. Sr-Nd ISOTOPE GEOCHEMISTRY

A total of 6 samples (3 Kfm and 3 rock samples) were subjected to Sr-Nd isotope analyses. The results are presented in table 3. However, in two of the Kfm samples (Kfm7 and Kfm20), it was not possible to measure Nd isotopes. The initial $^{87}Sr/^{86}Sr$ and $^{143}Nd/^{144}Nd$ ratios were calculated based on 70 Ma radiometric age results (Asutay, 1988; Kuşçu et al., 2007, 2010). The rock and mineral samples have differing isotope distributions. While the rock samples' initial $^{87}Sr/^{86}Sr$ varies between 0.70597-0.70628 and shows a wide range distribution, the Kfm samples' initial $^{87}Sr/^{86}Sr$ distribution varies between 0.70609-0.70610 and shows a short range. The $^{143}Nd/^{144}Nd$ ratios of the rock samples vary between 0.51238-0.51242 and differ from the ratios of the initial Sr isotope values by displaying a short range. $^{143}Nd/^{144}Nd$ value measured in one Kfm sample is 0.51243 and closer to the results obtained from the rock samples.

While the highest and lowest radiogenic samples contain $Sr_{(i)}$ from the rock samples (K5 =0.70597, K20= 0.70605), the most radiogenic samples contain $Nd_{(i)}$ from the Kfm sample (Kfm-12=0.51243).

When the rock and Kfm (1 sample) samples are evaluated in the initial Sr isotope and Nd (εNd) correlation diagrams (Fig. 5), it can be seen that rock and Kfm are similar and found in similar areas. The samples shown in Fig. 4a display an enriched lower crust with high Rb/Sr and low Sm/Nd values, but it is close to the mantle region and displays a distribution from the older crust towards the younger crust (Jahn et al., 1999; Khalaji et al., 2007). Similarly, in the $\varepsilon Nd\text{-}Sr_{(i)}$ diagram (Parada et al., 1999), the rock samples and mineral samples are located in similar areas and distributed in the lithospheric mantle area (Fig. 5b).

7. DISCUSSION AND CONCLUSIONS

7.1. Fractional Crystallization

Keban A-type syenitic rocks display similar petrographical and geochemical properties. Changes in quartz and mafic mineral contents, modal mineralogy and whole rock geochemistry are conformable. The whole rock geochemical data of the samples indicate that the magma composition was modified by the FC processes (Kürüm, 2012). A negative Ti anomaly (Fig. 3b) is an indication of Fe-Ti oxide fractionation (Zhou et al., 2004) and this is compatible with rocks sphene. The changes of the samples in the $^{87}Sr/^{86}Sr_{(i)}$ versus SiO_2, K_2O, Sr, Rb/Sr, La/Yb, Th and MgO with $^{143}Nd/^{144}Nd_{(i)}$ versus SiO_2, MgO, Nd and Sm/Nd diagrams were determined (Figs. 6a-j). According to these diagrams (Figs. 6b-f) in the Kfm samples, crystal fractionation is clearly observed. In these kinds of diagrams, nearly constant trends indicate FC while negative or positive trends indicate AFC (Kaygusuz et al., 2011).

Table 3. Sr and Nd isotope data from the Keban intrusive rocks and Kfms.

Sample	Rb (ppm)	Sr (ppm)	$^{87}Rb/^{86}Sr$	$^{87}Sr/^{86}Sr$	$^{87}Sr/^{86}Sr_i$	Nd (ppm)	Sm (ppm)	$^{143}Nd/^{144}Nd$	$^{143}Nd/^{144}Nd_i$	εNd
K-5 (syenite)	212	952	0.6446849	0.706609	0.7059680	53.0	7.72	0.512460	0.512420	-2.50
K-12 (syenite)	176	1485	0.3431111	0.706614	0.7062729	53.2	8.29	0.512431	0.512388	-3.12
K-20 (syenite)	158	1318	0.3470486	0.706397	0.7060520	46.9	6.76	0.512442	0.512402	-2.85
K-7 (Kfm)	198	2124	0.2698729	0.706372	0.7061038	5.5	0.89	-	-	-
K-12 (Kfm)	170	3100	0.1587581	0.706299	0.7061413	5.8	0.99	0.512480	0.512433	-2.25
K-20 (Kfm)	184	2530	0.2105455	0.706299	0.7060898	7.4	1.21	-	-	-

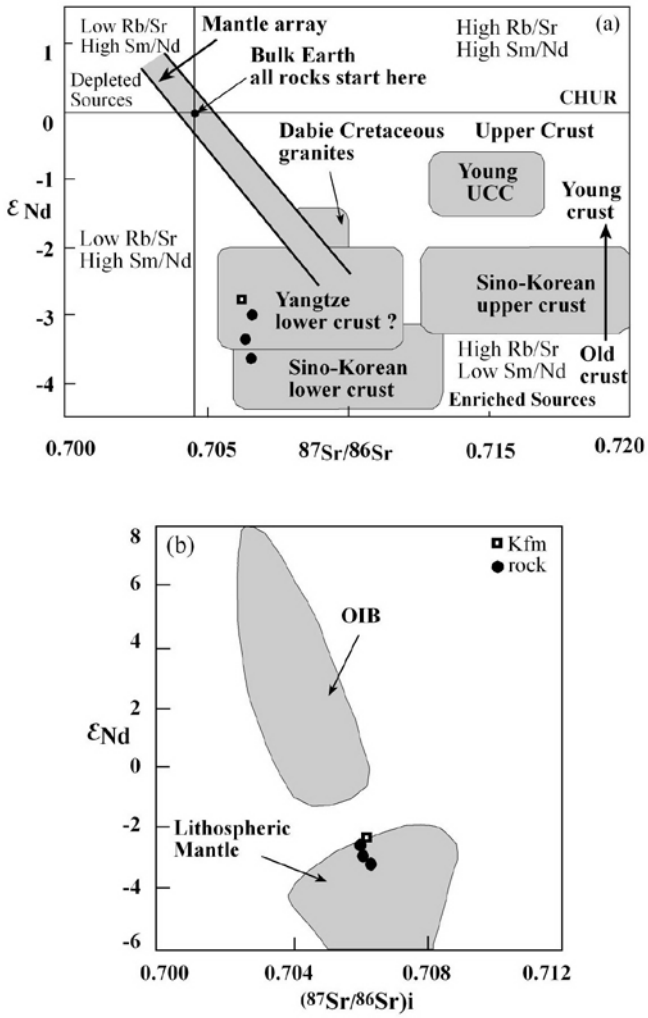

Figure 5. (a, b) εNd vs. initial 87Sr/86Sr plot for a variety of the A-type Keban syenitic rocks (from a: Jahn et al., 1999; Khalaji et al., 2007, b: Parada et al., 1999). (CHUR):Chondrite Uniform Reservoir, UCC: upper continental crust, OIB: oceanic island basalt.

While the element distribution of the rock samples in these diagrams predominantly indicates crustal contamination or AFC, for the distributions in the Kfm samples (especially in K_2O, Sr, Rb/Sr and La/Yb diagrams), fractionation is very distinct.

7.2. Source Characteristics

Geochemical and isotopic properties of the Keban A-type syenitic rocks were investigated in detail in order to determine their petrogenesis and source characteristics. The investigations revealed that enrichment in LILE, HFSE and LREE, and negative Nb, Ti anomalies (Fig. 4) are the distinctive geochemical characteristics of these rocks, and these results indicate typical subduction zone rocks. The Ba/Nb – La/Nb diagram (Fig. 7a) indicates that these rocks have properties of arc volcanics. The fact that these rocks have geochemical compositions of island arc indicates a subduction zone enrichment or crustal contamination (Boztuğ, 2008). This usually implies modification by the metasomatic fluids that originated from subducting slabs or sediments (Pearce, 1983; Elburg et al., 2003). The facts that the samples of the study area were found close to the medians of the clastic sediments and together with the granulites (Fig. 7a) support this view. Geochemically, for the formation of rocks to have these properties, a model was suggested that included a melting subcontinental mantle that was modified and enriched during the early stages of subduction (Kaygusuz et al., 2011). For this purpose, different elements ratio/ratio distributions of the rocks were studied (Pearce, 1982; Pearce et al., 1990). According to the studies, even if the distributions of the samples in the Ba/Nb-La/Nb diagram (Fig. 7a) (Jahn et al., 1999) indicates a multiple source, they are usually located in the area of island volcanics displaying granulitic properties. In the La/Nb-Ti diagram (Fig. 7b) (Pearce, 1982; Pearce et al., 1990), the samples are away from MORB and OIB, close to the subduction melts area and in the subduction zone magma (SZM) area. Such geochemical compositions displaying arc properties may reflect both subduction zone and intercontinental enrichment (Boztuğ, 2008). In the Rb/Y-Nb/Y diagram (Fig. 7c), the effects of the upper crust and/or within plate enrichment is clearly observed.

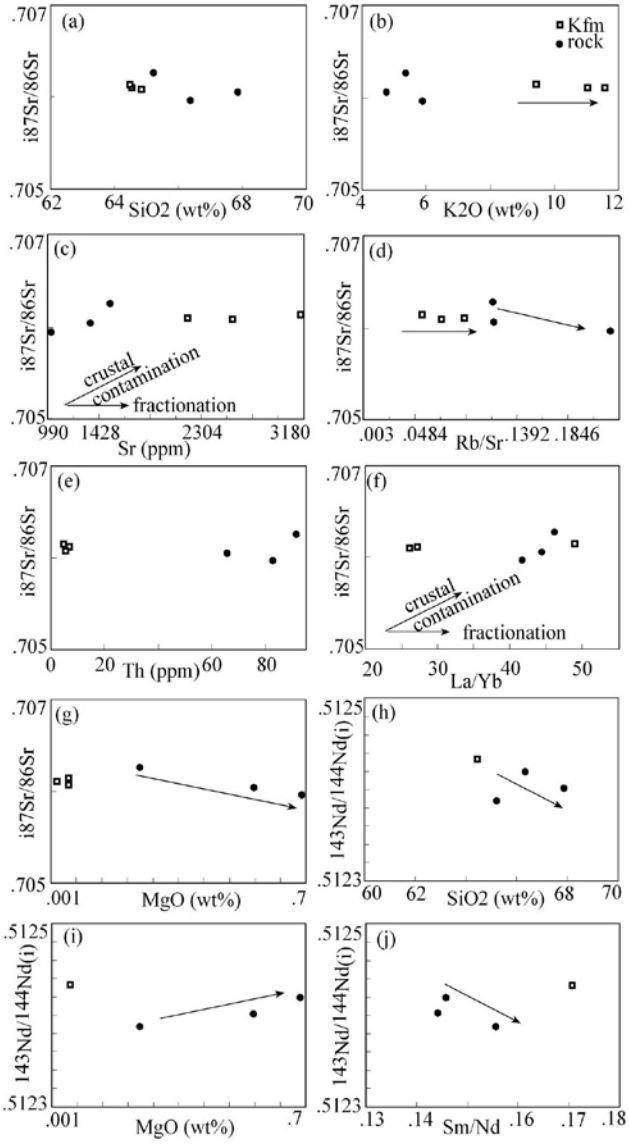

Figure 6. Variation of 87Sr/86Sr isotope ratio vs. SiO2 (wt%), K2O (wt%), Sr (ppm), Rb/Sr , La/Yb, Th (ppm) and MgO (wt%) (a-g), and 143Nd/144Nd isotope ratios vs. MgO (wt%), SiO2 (wt%) and Sm/Nd (h-j) for Keban A-type syenitic rocks. The 87Sr/86Sr and 143Nd/144Nd isotope ratios are plotted against the oxides and element ratios to evaluate the role of fractional crystallization (FC) or (AFC) processes and crustal contamination. Nd isotope ratios were measured for Kfms in a sample (K12) (Table 3).

These data is also conformable with the petrogenetical models suggested for the A-type granitoids. According to these models, A-type granitoids are formed by melting of crust and mantle (Kemp & Hawkesworth, 2003; Zhang et al., 2007; Karslı et al., 2012), by partial melting of a magma with crust and mantle origin (Bonin, 2007; Yang et al., 2006), or melting of the I-type granitoids or their residual sources (Turner et al., 1992). Similarly, geochemical properties in the Nb/La-La/Yb diagram (Fig. 7d), suggest Keban syenite porphyrs are affected by the fluid metasomatism formed by the lithospheric mantle and lithospheric-astenospheric mantle mixture, and geochemical properties of a subduction zone where continental contamination is effective are displayed. According to Boztuğ (2008), these rocks were originated from a metasomatic mantle source that originated from a previous subduction zone and was subjected to metasomatism by the fluids. In figure 7d, the fact that the majority of the samples are plotted in the lithospheric mantle area close to the lower crust is conformable with the other geochemical data. Similarly, in the Ba/Nb-La/Nb diagram (Fig.7a), the samples are plotted in the area of the arc volcanics, and Eastern Hebei Granulite with continental sediment property is in harmony with these data.

The geochemical data obtained from the A-type syenitic rocks are not distinct indications of crustal contamination processes. However, enrichment in elements such as K, Rb, Th and Ce shows the role of continental crust. The low contents of mafic components such as MgO (0.52%wt) and Ni (<20ppm) also reflect the effect of the continental crust. The average Ba/Nb values (54.26) (Table 1) are consistent with the continental crust values (54.00) (Rollinson, 1993). This also confirms the effect of the continental crust in this magmatism.

High Nb/La ratios indicate an OIB-like astenospheric mantle source for the basaltic magmas (Fig. 7d). Low Nb/La ratios (approximately <0.5) are accepted as an indicator of the lithospheric mantle source (Kaygusuz et al., 2011). However, despite the fact that a low Nb/La ratio indicates a lithospheric source, La enrichment in the source indicates metasomatism of the mantle source with the subduction fluids. Eby (1992) states that the value of the Y/Nb ratio is important in determining whether A-type granitoids are of mantle (Y/Nb<1.2) or crustal (Y/Nb>1.2) origin. In this respect, the Yb/Nb ratio of Keban syenitic rocks is smaller than 1.2 (0.49 in average). This indicates a mantle origin that is conformable with all the data presented above. Based on the geochemical data, it can be said that crustal contamination played an important role in the formation of A-type Keban syenitic rocks with a mantle source origin that was metasomatised by fluids. During the rise of magma shows differentiation and the lithospheric mantle characteristics.

When the La/Nb ratio of the samples is greater than 1.0 (Fig. 7a, b, d), the mantle source is likely litospheric (Boztuğ, 2008). The magma formed as a result of partial melting of such metasomatised lithospheric mantle source might be contaminated with the crustal material during its rise within the crust (Boztuğ, 2008). This is the reason

why FC plays an important role during the crystallisation of magmatic melt (Fig. 7e). Similarly, it is claimed that rocks with high-alkali content are formed by the partial melting of the subcontinental lithospheric mantle that is modified by the slabs made up of fluids or melts (Jiang et al., 2005).

It is also experimentally proven that interaction between the hydrous fluids and mantle gives rise to potassic magma formation (Jiang et al., 2005; Wyllie & Sekine, 1982). Douce (1997) performed melting experiments on tonalites and granodiorites with calc alkaline composition and stated that in the source of A-type granites, melt pressure was more important than the composition of the source material. He stated that plagioclase- and orthoclase-rich A-type granites crystallised under low pressure and had characteristic major and trace elements. Also, Jiang et al. (2009) stated that the source of the A-type plutons might be similar to that of I-type plutons depending on the partial meltings.

The high $^{87}Sr/^{86}Sr_{(i)}$ isotope ratios and negative εNd values in the rocks indicate a mantle source enriched with the subducting crustal material or material of crustal composition (Faure & Mensing, 2005).

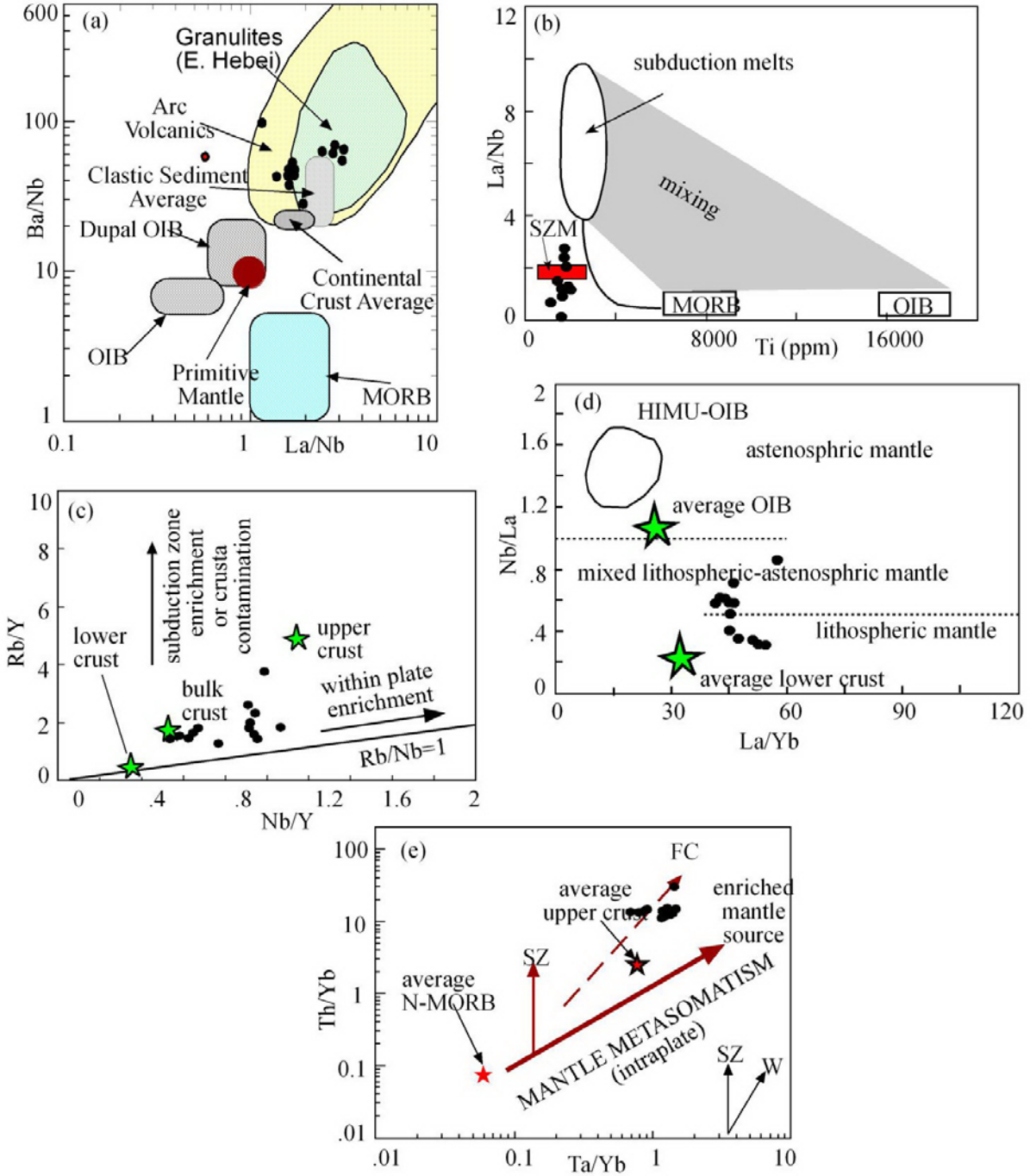

Figure 7. (a) Ba/Nb vs. La/Nb (Jahn et al., 1999), (b) La/Nb vs. Ti (Pearce, 1982; Pearce et al., 1990), (c) Rb/Y vs. Nb/Y (Pearce et al., 1990), (d) Nb/La vs. La/Yb (Kaygusuz et al., 2011, from Smith et al., 1999 and Weawer et al., 1987) and (e) Th/Yb vs. Ta/Yb (Pearce et al., 1990) plots of the A-type Keban syenitic rocks.

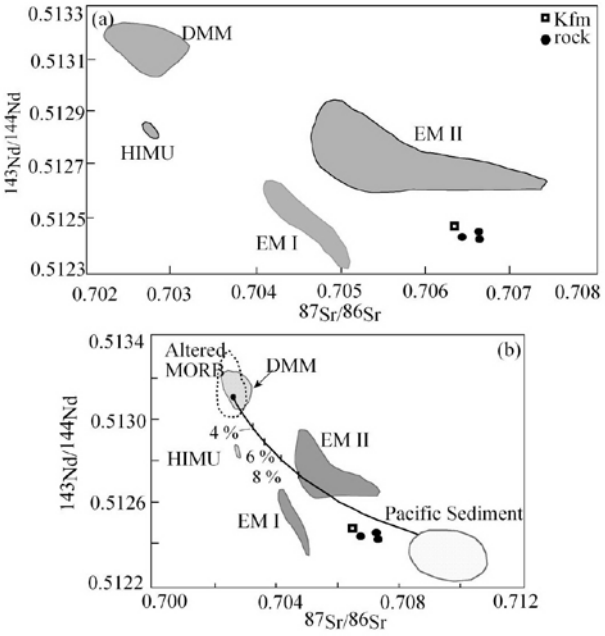

Figure 8. (a, b) Variation of 143Nd/144Nd and 87Sr/86Sr isotopes of the studied Keban A-type syenites, plotted on Machado et al., 2005. Abbreviations: EM: (Enriched Mantle), HIMU: (High μ), DMM: (Depleted Mantle). Line represents a mixing between altered MORB (DMM field) and sediments (Pacific sediments filed). It indicates the bulk mixture between 4 wt.% of sediment and 96 wt.% of altered MORB (b).

Mineral and rock samples of the study area located between EM I and EM II - Pacific sediments (Fig. 8b) in the $^{87}Sr/^{86}Sr$-$^{143}Nd/^{144}Nd$ isotope diagrams (Figs. 8a, b) indicate an enriched source region and the effect of the pelagic sediments. The fact that the samples are located in the lower (older) crust area supports the above result. This situation may be explained by the recycling of the oceanic crust and overlying pelagic sediments or the delamination or thermal ionisation of the subcontinental lithosphere, or via the lithosphere metosomatism during the subduction processes (Machado et al., 2005). The Sr-Nd isotope concentration in the Keban syenite and Kfms in figures 5-8 can be explained by the contamination of the magma with the lithospheric fluids causing enrichment in Sr and LILEs. This is as a result of the dehydration of the clastic sediments and secondarily pelagic sediments (EM I) during the subduction process (EM II). When considered along with the values of Sr-Nd isotopes and εNd, it can be understood that oceanic crust did not contribute to the isotopic composition of the source. It is suggested that the recycling of the continental crust are effective for the source with EM II composition (Zindler & Hart, 1986). The fact that the values of εNd are similar to each other in the Kfm and in the rock samples (Table 3) indicates that the source magma is not modified with time during the formation of minerals and rocks (Machado et al., 2005).

7.3. Geodynamic Interpretation

The distribution of the Keban A-type syenitic rocks in the Batchelor and Bowden (1985) and the Pearce et al. (1984) geotectonic discrimination diagrams (Figs. 9a-c) indicates that they are of late orogenic (Fig. 9a) and WPG (Figs. 9b, c) character. Pearce (1996) suggests that the post-collision granitoids may display WPG, syn-COLG, VAG features. It is recorded that similar geodynamic properties are observed in the A-type granitoids of Central Anatolia (Boztuğ, 1998; Düzgören-Aydın et al., 2001; Köksal & Göncüoğlu, 2007).

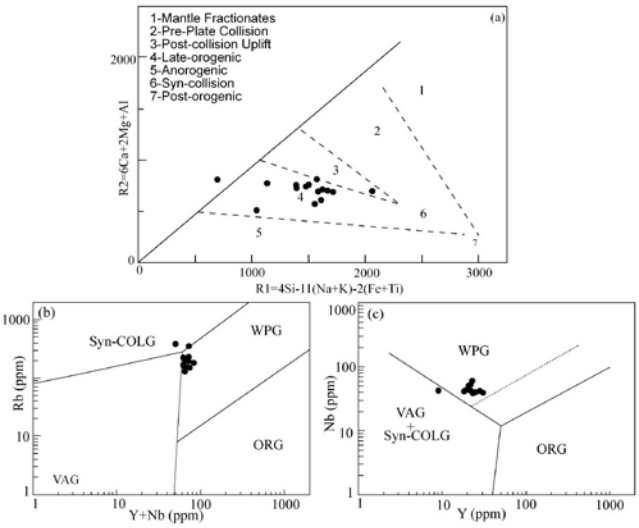

Figure 9. (a) R1-R2 Batchelor and Bowden (1985) major element plot. (b) Rb-(Y+Nb), (c) Nb-Y tectonic discrimination plot (Pearce et al., 1984) for the studied Keban A-type syenites. Majority of the ratios fall in WPG area in (a) and (b). Syn-COLG, syn-collisional granitoids; WPG, within-plate granitoids; VAG, volcanic-arc granitoids; ORG, ocean-ridge granitoids.

The researchers stated that these granitoids were formed in the post-collisional and subsequent extensional environments. The above mentioned geotectonic properties, evaluated together with all the field and geochemical data obtained by considering the Keban syenitic rocks within the concept of Eurasia and Taurid-Anatolide collision zone could be interpreted to be the result of the post-collisional magmatism. The petrogenetic and geodynamic properties of Keban A-type syenitic rocks display similarities with the Çamsarı A-type granitoids of Central Anatolia (properties such as subcontinental litospheric enrichment, dehydration, and melting of the sediments or basaltic crust) (Köksal et al., 2004; Köksal & Göncüoğlu, 2007). It is known that the origin of the magmatism related to the subduction in Eastern-Southeastern Anatolia is directly connected with the closing of Neothethys Ocean. Kuşçu et al. (2010), states that the post-collisional and late

orogenic interplate magmatism is the result of the collision between the ophiolitic rocks coming from the north and southeast Anatolian orogenic belt.

8. CONCLUSIONS

In conclusion, the data obtained from the field work, mineral and whole rock geochemistry and isotope analyses, indicates that this porphyric pluton-bearing K-feldspar megacrystal is an A-type pluton that was formed by a magma that originated from the partial melting of litospheric mantle and lower crust. These were enriched by the metasomatised early subduction fluids in a post-collisional environment. During crystallization of magma FC, AFC and crustal contamination has been effective. The fact that Kfms display similar isotopic properties with the host rock indicates that the source magma was not modified during solidification.

ACKNOWLEDGMENTS

This paper is part of a project supported by FUBAP of Fırat University (Project Number-1948), Elazığ, Turkey. The author kindly thanks Dr. Serhat Köksal (METU, Ankara, Turkey) for the Sr and Nd isotope analysis determination and is especially indebted to Prof. Hakan Çoban for his corrections and detailed comments.

REFERENCES

Asutay, H.J., 1988. *Geologic and petrografic studies around of Baskil (Elazığ).* MTA Bull. 107, 38–60. (In Turkish with English abstract)

Batchelor, B. & Bowden, P., 1985. *Petrogenetic interpretation of granitoid rock series using multicationic parameters.* Chemical Geology, 48, 43–55.

Bonin, B., 2007. *A-type granites and related rocks: evolution of a concept problems and prospects.* Lithos, 97, 1–29.

Boztuğ, D., 1998. *Post-collisional central Anatolian alkaline plutonism, Turkey.* Turkish Journal of Earth Sciences, 7, 145–165.

Boztuğ, D., 2008. *Petrogenesis of the Kösedağ Pluton, Suşehri-NE Sivas, East-Central Pontides, Turkey.* Turkish Journal of Earth Sciences, 17, 241–262.

Çalık, A. & Öngen, S., 1998. *Keban magmatics: mineralogy, petrology and the contact zone of the Sarılımagara syenite porphry.* Third International Turkish Geology Symposium Work in Progress on the Geology of Turkey and its surroundings, Middle East Technical University, Ankara, Abstract. 129.

Douce, A.E.P., 1997. *Generation of metaluminous A-type granites by low-pressure melting of calcalkaline granitoids.* Geology, 25(8), 743-746.

Düzgören-Aydın, N., Malpas, W., Göncüoğlu, M.C. & Erler, A., 2001. *A review of the nature of magmatism in central Anatolia during the Mesozoic post-collisonal period.* International Geology Review, 43, 695–710.

Eby, G.N., 1990. *The A-type granitoids: a review of their occurrence and chemical characteristics and speculation on their petrogenesis.* Lithos, 26, 115–134.

Eby, G.N., 1992. *Chemical subdivision of the A-type granitoids: petrogenesis and tectonic implications.* Geology, 20, 641–644.

Elburg, M.A., Van Bergen, M.J. & Foden, J.D., 2003. *Subducted upper and lower continental crust contributes to magmatism in the collision sector of the Sunda-Banda arc, Indonesia.* Geological Society of America, 32, 41-44.

Faure, G. & Mensing, T.M., 2005. *Isotopes: Principles and Applications.* John Wiley & Sons, 897pp.

Jahn, B-M., Wu, F., Lo, C-H. & Tsai, C-H., 1999. *Crust mantle interaction induced by deep subduction of the continental crust: geochemical and Sr–Nd isotopic evidence from post-collisional mafic–ultramafic intrusions of the northern Dabie complex, central China.* Chemical Geology, 157, 119–146.

Jiang, Y.H., Ling, H.F., Jiang, S.Y., Fan, H.H., Shen, W.Z. & Ni, P., 2005. *Petrogenesis of a late Jurassic peraluminous volcanic complex and its high-Mg, potassic quenched enclaves at Xianshan, Southeast China.* J. Petrol., 46, 1121–1154.

Jiang, N., Zhang, S. & Zhou, W., 2009. *Origin of a Mesozoic granite with A-type characteristics from the North China craton: highly fractionated from I-type magmas?* Contrib. Mineral. Petrol., doi:10.1007/s00410-008-0373-2.

Karslı, O., Caran, Ş., Dokuz, A., Çoban, H., Bin Chen, B. & Kandemir, R., 2012. *A-type granitoids from the Eastern Pontides, NE Turkey: Records for generation of hybrid A-type rocks in a subduction-related environment.* Tectonophysics, 530–531, 208–224.

Kaygusuz, A., Arslan, M., Siebel, W. & Şen, C., 2011. *Geochemical and Sr-Nd isotopic characteristics of post-collisional calc-alkaline volcanic in the Eastern pontides (NE Turkey).* Turkish Journal of Earth Sciences, 20, 137-159.

Kemp, A.I.S. & Hawkesworth, C.J., 2003. *Granitic perspectives on the generation and secular evolution of the continental crust.* Treatise Geochem., 3, 349–410.

Khalaji, A.A., Esmaeily, D., Valizadeh, M.V. & Rahimpour-Bonab, H., 2007. *Petrology and geochemistry of the granitoid complex of Boroujerd, Sanandaj-Sirjan Zone, Western Iran.* Journal of Asian Earth Sciences, 29, 859–877.

Kipman, E., 1983.*The petrology of the Keban volcanic.* Istanbul. Univ. Earth Sci., 3(4), 205-230.

Köksal, S., Romer, R.L., Göncüoğlu, M.C. & Toksoy-Köksal, F., 2004. *Timing of post-collisional H-type to A-type granitic magmatism: U-Pb titanite ages from the Alpine central Anatolian granitoids (Turkey).* Int. J. Earth Sci., 93, 974–989.

Köksal, S. & Göncüoğlu, M.C., 2007. *Sr and Nd Isotopic Characteristics of Some S-, I- and A-type Granitoids from Central Anatolia.* Turkish Journal of Earth Sciences, 17, 111–127.

Kuşcu, İ., Gençalioğlu-Kuşcu, G., Tosdal, R.M., Ullrich, T. & Friedman, R., 2007. *Link between magmatism and subduction-related events in southeastern Turkey.* European Geosciences Union 2007, Geophysical Research, Abstracts 9: A-04814.

Kuşcu, İ., Gençalioğlu-Kuşcu, G., Tosdal, R.M., Ullrich, T. & Friedman, R., 2010. *Magmatism in the southeastern Anatolian orogenic belt: transition from arc to post-*

collisional setting in an evolving orogen. In: Sosson, M., Kaymakcı, N., Stephenson, R.A., Bergerat, F., Starostenko, V. (Eds) *Sedimentary Basin Tectonics from the Black Sea and Caucasus to the Arabian Platform.* Geological Society, London, Special Publications, 437–460

Kürüm, S., 2012. *Mineral chemistry of K-feldispar megacrystals and petrochemistry of the Keban syenitic intrusives, Elazığ, Eastern-Turkey.* Scientific Research and Essays, 7-40, 3442-3457.

MacKenzie, W.S., Donaldson, C.H. & Guilford, C., 1982. *Atlas of Igneous Rocks and their Textures*. Longman Group Ltd., Essex, pp 148.

Machado, A., Chemale, F. Jr., Conceic, R.V., Kawaskita, K., Morata, D., Oteiza, O. & Van Schmus, W.R., 2005. *Modeling of subduction components in the genesis of the Meso-Cenozoic igneous rocks from the South Shetland Arc, Antarctica*. Lithos, 82, 435– 453.

Martin, R.F., 2006. *A-type granites of crustal origin ultimately result from open-system fenitization type reactions in an extensional environment.* Lithos, 91, 125-136.

Parada, M.A., Nystro, J.O. & Levi, B., 1999. *Multiple sources for the Coastal Batholith of central Chile (31–34^{0}S): geochemical and Sr–Nd isotopic evidence and tectonic implications*. Lithos, 46, 505–521.

Parlak, O., 2006. *Geodynamic significance of granitoid magmatism in the southeast Anatolian Orogen: geochemical and geochronogical evidence from Göksun–Afşin (Kahramanmaraş, Turkey) Region.* International Journal of Earth Sciences, 95, 609–627.

Pearce, J.A., 1982. *Trace element characteristics of lavas from destructive plate boundaries. In: Thorpe, R.S. (Ed), Andesites*. Wiley, New York, 525–548.

Pearce, J.A., 1983. *Role of the sub-continental lithosphere in magma genesis at active continental margins.* In: Hawkesworth, C.J., Norry, M.J. (Eds), *Continental Basalts and Mantle Xenoliths*, Shiva Publications, 230-249.

Pearce, J., 1996. *Sources and settings of granitic rocks.* Episodes, 19-4, 120-125.

Pearce, J.A., Harris, N.B.W. & Tindle, A.G.W., 1984. *Trace element discrimination diagrams for the tectonic interpretation of granitic rocks.* Journal of Petrology, 25, 956–983.

Pearce, J.A., Bender, J.F., De Long, S.E., Kidd, W.S.F., Low, P.J., Güner, Y., Şaroğlu, F., Yılmaz, Y., Moorbath, S. & Mitchell, J.G., 1990. *Genesis of collision volcanism in Eastern Anatolia, Turkey.* Journal of Volcanology and Geothermal Research, 44, 189–229.

Peccerillo, A. & Taylor, S.R., 1976. *Geochemistry of the calc-alkaline volcanic rocks from the Kastamonu area, Northern Turkey*. Contrib Mineral Petrol., 58, 63–81.

Rızaoğlu, T., Parlak, O., Höck, V., Koller, F., Hames, W.E. & Billor, Z., 2008. *Andean Type Active Margin Formation in the Eastern Taurides: Geochemical and Geochronological Evidence from the Baskil Granitoid, SE Turkey*. Tectonophysics, 473(1-2), 188-207.

Romer, R.L., Forster, H-J. & Breıtkreuz, C., 2001. *Intracontinental extensional magmatism with a subduction fingerprint: the late Carboniferous Halle Volcanıc Complex (Germany).* Contributions to Mineralogy and Petrology, 141, 201–221.

Rollinson, H., 1993. *Using Geochemical Data: Evaluation, Presentation, Interpretation.* Longman Group, UK, 352 pp.

Smith, E.I., Sanchez, A., Walker, J.D. & Wang, K., 1999. *Geochemistry of mafic magmas in the Hurricane Volcanic field, Utah: implications for small- and large-scale chemical variability of the lithospheric mantle.* Journal of Geology, 107, 433–448.

Sun, S.S. & McDonough, W.F., 1989. *Chemical and isotopic systematics of oceanic basalts: Implications for mantle composition and processes.* In: Saunders, A.D., Norry, M.J. (Eds.) *Magmatism in the Ocean Basins*. Geological Society Special Publication, 42, 313–345.

Sylvester, P.J., 1989. *Post-collisional alkaline granites.* The Journal of Geology, 97-3, 261-280.

Turner, S.P., Foden, J.D. & Morrison, R.S., 1992. *Derivation of some A-type magmas by fractionation of basaltic magma; an example from the Padthaway Ridge, South Australia*. Lithos, 28, 151–179.

Vernon, R.H., 1986. *K-Feldspar megacrysts in granites phenocrysyts, not porphyroblasts.* Earth Science Reviews, 23, 1–63.

Whalen, J.B., Currie, K.L. & Chappell, B.W., 1987. *A-type granites: geochemical characteristics, discrimination and petrogenesis.* Contrib. Mineral. Petrol., 95, 407–419.

Wyllie, P.J. & Sekine, T., 1982. *The formation of mantle phlogopite in subduction zone hybridzation.* Contrib. Mineral. Petrol., 79, 375-380.

Yang, J.H., Wu, F.Y., Chung, S.L., Wilde, S.A. & Chu, M.F., 2006. *A hybrid origin for the Qianshan A-type granite, northeast China: geochemical and Sr–Nd–Hf isotopic evidence.* Lithos, 89, 89–106.

Yılmaz, Y., 1993. *New evidence and model on the evolution of the Southeast Anatolian Orogen.* Geological Society of America Bulletin, 105, 251-271

Zhang, H.F., Parrish, R., Zhang, L., Xu, W.C., Yuan, H.L., Gao, S. & Crowley, Q.G., 2007. *A-type granite and adakitic magmatism association in Songpan–Garze fold belt, eastern Tibetan Plateau: implication for lithospheric delamination.* Lithos, 97, 323–335.

Zhou J., Wang, X.,Qıu, J. & Gao, J., 2004. *Geochemistry of Meso- and Neoproterozoic mafic-ultramafic rocks from northern Guangxi, China: Arc or plume magmatism?.* Geochemical Journal, 38,. 139-152.

Zindler, A. & Hart, S.A., 1986. *Chemical geodynamics.* Annu. Rev. Earth Planet Sci., 14, 493– 571.

Received at: 04. 02. 1013
Revised at: 12. 10. 2013
Accepted for publication at: 18. 10. 2013
Published online at: 26. 10. 2013